Research Article

Pardis Ghahramani, Kamran Behdinan*, Rasool Moradi-Dastjerdi, and Hani E. Naguib

Theoretical and experimental investigation of MWCNT dispersion effect on the elastic modulus of flexible PDMS/MWCNT nanocomposites

https://doi.org/10.1515/ntrev-2022-0006
received August 17, 2021; accepted October 22, 2021

Abstract: In this article, Young's modulus of a flexible piezoresistive nanocomposite made of a certain amount of multiwalled carbon nanotube (MWCNT) contents dispersed in polydimethylsiloxane (PDMS) has been investigated using theoretical and experimental approaches. The PDMS/MWCNT nanocomposites with the governing factor of MWCNT weight fraction (*e.g.*, 0.1, 0.25, and 0.5 wt%) were synthesized by the solution casting fabrication method. The nanocomposite samples were subjected to a standard compression test to measure their elastic modulus using Instron Universal testing machine under force control displacement mode. Due to the costs and limitations of experimental tests, theoretical predictions on the elasticity modulus of such flexible nanocomposites have also been performed using Eshelby–Mori–Tanaka (EMT) and Halpin–Tsai (HT) approaches. The theoretical results showed that HT's approach at lower MWCNT contents and EMT's approach at higher MWCNT contents have a better agreement to experimental results in predicting the elastic modulus of PDMS/MWCNT nanocomposites. The experimental results indicated that the inclusion of MWCNT in the PDMS matrix resulted in a noticeable improvement in Young's modulus of PDMS/MWCNT nanocomposite at small values of MWCNT contents (up to w_f = 0.25%); however, exceeding this nanofiller content did not elevate Young's modulus due to the emergence of MWCNT agglomerations in the nanocomposite structure.

Keywords: flexible PDMS-MWCNT nanocomposite, Young's modulus, compression test, theoretical approaches, CNT agglomeration, CNT aspect ratio

1 Introduction

Development of novel flexible highly sensitive pressure-detecting sensors with high durability, biocompatibility, and lightweight has drawn tremendous attention toward smart systems and wearable healthcare devices [1–4]. Flexible piezoresistive nanocomposite sensors are a type of pressure-sensitive sensor whose applications in biomedical science have been gradually increased over the last decade [5–9]. Piezoresistive effect is a change in the electrical resistance of a material when mechanical strain is applied to it. Piezoresistive nanocomposite sensors are built up from a polymeric matrix and a reinforcement phase, which their work principle counts on resistivity change due to the displacement of conductive networks inside their structure in response to an external force. Controlling the elastic modulus of nanocomposites is the key factor in the design of flexible piezoresistive nanocomposites, which has a crucial impact on both their electrical and mechanical responses [10,11]. In this regard, multiwalled carbon nanotubes (MWCNTs) have attracted great interest to be used in nanocomposites owing to their exceptional electronic and mechanical characteristics, which include tremendously high elastic modulus, low density, large surface area, and high aspect ratio [12–15]. The elastic modulus of a nanocomposite is a function of many parameters including the polymer elasticity, weight fraction, dispersion, agglomeration fraction, and aspect ratio of reinforcement particles along with the bonding between polymer and reinforcement particles [16]. Therefore, many endeavors have been performed to investigate the elastic modulus of nanocomposite materials with

* **Corresponding author: Kamran Behdinan,** Advanced Research Laboratory for Multifunctional Lightweight Structures (ARL-MLS), Department of Mechanical & Industrial Engineering, University of Toronto, Toronto, Canada, e-mail: Behdinan@mie.utoronto.ca
Pardis Ghahramani, Rasool Moradi-Dastjerdi: Advanced Research Laboratory for Multifunctional Lightweight Structures (ARL-MLS), Department of Mechanical & Industrial Engineering, University of Toronto, Toronto, Canada
Hani E. Naguib: Toronto Smart Materials and Structures (TSMART), Department of Mechanical & Industrial Engineering, University of Toronto, Toronto, Canada, e-mail: Neguib@mie.utoronto.ca

different polymeric matrices enhanced with single- or multiwalled CNTs.

Different numerical/theoretical approaches, such as molecular dynamic (MD) simulations, Eshelby–Mori–Tanaka (EMT), Halpin–Tsai (HT), and the rule of mixture, have been proposed for the estimation of mechanical properties of nanocomposites. In MD simulations, the interactions between the atoms of the material are described by atomistic potentials based on the energy minimization of the system [17,18]. MD principles stand with the simulation of particles' motions in the presence of applied forces to the system. The potentials of chemical bonds between the atoms, which depend on the atomic distances, are responsible for the existing forces. It is worth mentioning that the length and timescale that can be explored in the MD simulation are limited. Usually, the size of the simulation varies from 10 Å to 100 nm, and the time step is 100 ns to microseconds [17]. The number of atoms that can be probed in the MD simulation is several thousand to millions. Moreover, the time step in the simulation should be considered long enough to minimize the computational costs, which will challenge the accuracy of the simulation in this case. Another limitation of using MD simulation is finding a proper forcefield in molecular mechanics to cover all the existing interactions will be a challenge [17]. Moreover, in these mixed phases, a larger quantity of particles in the simulation box should be considered to be representative enough for the system, which adversely adds to the computational time and cost.

Among the theoretical approaches, EMT, HT, and some modified forms of the rule of mixture have widely been used for the investigation of the nanoscale effect on CNT-reinforced nanocomposites. Although the rule of mixture offers a transversely isotropic nanocomposite material, the other two approaches assume that the resulting nanocomposite is an isotropic material. Shen [19] modified the micromechanical form of the rule of mixture by incorporating three parameters efficiency coefficients to capture the nanoscale effects of CNTs. He evaluated those coefficients by equaling the elastic modulus of CNT-reinforced nanocomposites from MD simulations with the original rule of mixture. However, this approach needs a set of coefficients for each type of material at desired temperatures or nanofiller volume fractions. Using the same concept, this micromechanical method was also further modified to involve the effects of the aspect ratio and waviness of the nanofiller part [20–23]. Halpin–Tsai model is also heavily used for nanocomposites. This model predicts the elasticity behavior of unidirectional composites/nanocomposites as a function of the filler's aspect ratio where the transverse and longitudinal Young's moduli are presented based on filler geometry and the loading direction [16]. For composites/nanocomposites with short fibers, another version of this approach was also introduced, which proposes an isotropic material [16,24,25]. To involve the impacts of nanofillers' orientation and agglomeration, EMT's approach has widely been used. In CNT-reinforced nanocomposites, CNT agglomeration is caused by intrinsic van der Waals interactions between nanoparticles. The other reasons for creating local CNT agglomerations in CNT-reinforced nanocomposites are the high aspect ratio, low bending rigidity, and high volume fraction of these nanotubes embedded in a polymer host [26]. It has been proven that CNT local aggregations significantly reduced the CNT functionalization [27,28]. Montazeri *et al.* [29] modified HT formulation based on some experimental tensile test outcomes to capture the agglomeration effect on the stiffness of an epoxy/MWCNT nanocomposite. They noticed that above 1.5 wt%, adding nanotubes could not improve the elasticity modulus of that nanocomposite due to MWCNT agglomerations. Barai and Weng [30] also used Mori–Tanaka approach on the small scale of a new two-scale theoretical model to study the agglomeration effect on the elastic and plastic behavior of CNT-reinforced polymeric nanocomposites. To introduce a lead-free piezoelectric nanocomposite material, Krishnaswamy *et al.* [31] added a lead-free piezoelectric inclusion inside a polydimethylsiloxane (PDMS)/CNT nanocomposite. They developed a modified micromechanical (EMT) approach to study the effect of CNT defect and agglomeration on the electro-mechanical properties of such active nanocomposites.

Besides the theoretical approaches, many experimental studies have been done to study the mechanical properties of nanocomposites. In a research article, Lu *et al.* [32] explored the effect of CNT content on the elastic modulus of a polymeric nanocomposite. They illustrated that by increasing the filler content in PDMS/CNT matrix up to a specific amount, Young's modulus of the nanocomposite increased. Due to the higher strength of conductive filler than polymer matrix, a higher filler ratio increased Young's modulus of the nanocomposite [33]. However, after a certain degree, the lower content of the polymer matrix inside the nanocomposite made the nanocomposite fragile and reduced its strength [34]. Madaleno *et al.* [35] observed that the compressive modulus and strength of polyurethane (PU)/CNT foam nanocomposite were enhanced in comparison to the pure PU foam. Tanabi and Erdal [34] studied the CNT dispersion effect on the mechanical properties of epoxy/CNT nanocomposites. Moreover, the effects of CNT dispersion [36–38], particles

agglomeration [39,40], and interfacial bonding between polymer matrix and filler [41] on the mechanical properties of CNT-reinforced composites have been investigated experimentally.

PDMS [5], polylactic acid [42], polyvinylidene fluoride, polycaprolactone [43], and polyaniline [44] are polymers that are largely used in the fabrication of nanocomposites for biomedical applications. PDMS has been overwhelmingly used as the polymer matrix in the flexible nanocomposites in comparison to the other types of flexible polymers [45–47]. PDMS has excellent advantages such as commercial availability, variable mechanical properties, transparency, chemical inertness, high flexibility, stability over a wide range of temperatures, and biocompatibility [48,49]. The outstanding attributes of PDMS and MWCNT made them a good candidate to be used as the main components for the fabrication of a soft piezoresistive nanocomposite with potential application as a biocompatible sensor in this research article [14].

In this article, Young's modulus of flexible PDMS/MWCNT nanocomposites as an essential mechanical parameter has been investigated using a standard compression experimental test at various MWCNT weight fractions, whereas the nanocomposite samples were fabricated by the solution casting method. In this method, the polymer matrix is added to a solution of dispersed particles in a solvent. Then the mixture gets homogenized by mixing at elevated temperature to evaporate the solvent. In the next step, a curing agent for crosslinking the polymer matrix is added to the mixture and poured in a mold. At the end of the process, mold will be put inside the oven to cure and solidify the nanocomposite structure.

For further understanding of the mechanical behavior of such nanocomposites and optimizing the use of nanoreinforcements, two theoretical (*i.e.*, EMT and HT) approaches were also used to predict the elasticity modulus while distribution and shape parameters of the reinforcement part are considered.

2 Theoretical approaches

Due to the reliable results of EMT and HT approaches, we used these two approaches for the elastic modulus estimation of PDMS/MWCNT nanocomposite. EMT's approach is able to consider random orientations for MWCNTs and their possible clustering. However, HT approach involves the geometrical dimension of the reinforcement part to consider its nanoscale effects.

2.1 EMT approach

According to the EMT approach, three types of nanofiller distribution including fully dispersed with aligned CNTs, fully dispersed with randomly oriented CNTs, and locally aggregated CNTs with random orientations can be considered. However, the first case is unlikely to happen because of the small bending rigidity and high aspect ratio of CNTs. Therefore, this subsection provides the formulations that cover the second and third types of CNT distributions in a polymeric matrix. It is worth mentioning that the fully dispersed type of nanocomposite is a specific condition of the nanocomposite with locally aggregated CNTs such that the whole volume of agglomerations and the volume of the nanocomposite are equal.

To investigate the negative impact of agglomerations on the elastic constants, Shi *et al.* [26] considered representative volume elements (RVEs) including a matrix with partly dispersed CNTs in agglomerations and partly well dispersed as shown in Figure 1. To generalize the RVE, they defined two parameters, which indicated the agglomeration volume μ and CNT concentration in those agglomerations η, which their definitions are mathematically presented in equation (1) [26]:

$$\mu = V_{\text{aggl.}}/V, \eta = f_{\text{r}}^{\text{aggl.}}/f_{\text{r}} \quad 0 \le \mu, \eta \le 1 \text{ and } \mu < \eta, \tag{1}$$

where f_{r} and $f_{\text{r}}^{\text{aggl.}}$ are the whole MWCNT volume fraction and MWCNT volume fraction embedded inside the agglomerations, respectively. In addition, the physical parameters of V and $V_{\text{aggl.}}$ are the whole volume (area) of RVE and the total volume (area) of the agglomerations, respectively. Due to the physical constraints, μ is always less than η. Moreover, cases with $\mu = 1$ or $\mu = \eta$ indicate RVE or nanocomposite with fully dispersed MWCNTs. Furthermore, $\eta = 1$ implies that whole MWCNTs are absorbed into each other, and there are no MWCNTs outside the agglomerations.

After generalizing this method for all possible agglomeration states, the mechanical properties of inside and

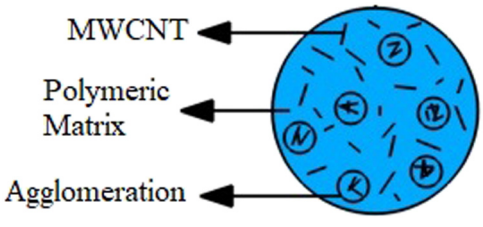

Figure 1: An EMT's RVE, which shows randomly oriented MWCNTs and their agglomerations, are dispersed in a polymeric matrix.

outside agglomerations can be evaluated separately. The shear G and bulk K moduli of the RVE can be determined using the corresponding values of the inside ($_{in}$) and outside ($_{out}$) of agglomerations as shown in equation (2) [26]:

$$\begin{aligned} K &= K_{out}\left[1+\frac{\mu\left(\frac{K_{in}}{K_{out}}-1\right)}{1+\alpha(1-\mu)\left(\frac{K_{in}}{K_{out}}-1\right)}\right], \\ G &= G_{out}\left[1+\frac{\mu\left(\frac{G_{in}}{KG_{out}}-1\right)}{1+\beta(1-\mu)\left(\frac{G_{in}}{G_{out}}-1\right)}\right], \end{aligned} \tag{2}$$

where

$$\alpha=\frac{1+\upsilon_{out}}{3(1-\upsilon_{out})},\quad \beta=\frac{2(4-5\upsilon_{out})}{15(1-\upsilon_{out})}, \tag{3}$$

$$\begin{aligned} K_{in} &= K_m+\frac{f_r\eta(\delta_r-3K_m\alpha_r)}{3(\mu-f_r\eta+f_r\eta\alpha_r)}, \\ K_{out} &= K_m+\frac{f_r(1-\eta)(\delta_r-3K_m\alpha_r)}{3[1-\mu-f_r(1-\eta)+f_r(1-\eta)\alpha_r]}, \end{aligned} \tag{4}$$

$$\begin{aligned} G_{in} &= G_m+\frac{f_r\eta(\eta_r-3G_m\beta_r)}{2(\eta_r-3G_m\beta_r)}, \\ G_{out} &= G_m+\frac{f_r(1-\eta)(\eta_r-2G_m\beta_r)}{2[1-\mu-f_r(1-\eta)+f_r(1-\eta)\beta_r]}. \end{aligned} \tag{5}$$

In equations (3)–(5), υ_{out} is the Poisson's ratio of outside of agglomerations and subscripts m and r are used to show the properties of the matrix and nanofiller materials, respectively. Moreover, α_r, β_r, δ_r, and η_r are defined as follows:

$$\alpha_r=\frac{3(K_m+G_m)+k_r-l_r}{3(K_m+k_r)}, \tag{6}$$

$$\begin{aligned} \beta_r=\frac{1}{5}\Bigg\{&\frac{4G_m+2k_r+l_r}{3(G_m+k_r)}+\frac{4G_m}{G_m+p_r} \\ &+\frac{2[G_m(3K_m+G_m)+G_m(3K_m+7G_m)]}{G_m(3K_m+G_m)+m_r(3K_m+7G_m)}\Bigg\}, \end{aligned} \tag{7}$$

$$\delta_r=\frac{1}{3}\left\{n_r+2l_r+\frac{(2k_r+l_r)+(3K_m+2G_m-l_r)}{G_m+k_r}\right\}, \tag{8}$$

and

$$\begin{aligned} \eta_r=\frac{1}{5}\Bigg[&\frac{2}{3}(n_r-l_r)+\frac{8G_mp_r}{G_m+p_r} \\ &+\frac{8m_rG_m(3K_m+4G_m)}{3K_m(m_r+G_m)+G_m(7m_r+G_m)} \\ &+\frac{2(k_r-l_r)(2G_m+l_r)}{3(G_m+k_r)}\Bigg], \end{aligned} \tag{9}$$

where k_r, m_r, l_r, p_r, and n_r denote Hill's elastic moduli of nanofiller, which can be found by matching the following (Hill's) elastic matrix with the elastic stiffness matrix for MWCNT [26,50,51].

$$C_r=\begin{bmatrix} n_r & l_r & l_r & 0 & 0 & 0 \\ l_r & k_r+m_r & k_r-m_r & 0 & 0 & 0 \\ l_r & k_r-m_r & k_r+m_r & 0 & 0 & 0 \\ 0 & 0 & 0 & p_r & 0 & 0 \\ 0 & 0 & 0 & 0 & m_r & 0 \\ 0 & 0 & 0 & 0 & 0 & p_r \end{bmatrix}. \tag{10}$$

As mentioned before, EMT's approach assumes that the resulting nanocomposite is an isotropic material. Therefore, by obtaining K and G from equation (2), Young's modulus of PDMS/MWCNT nanocomposite will be defined according to equation (11):

$$E=\frac{9KG}{3K+G}. \tag{11}$$

2.2 Halpin–Tsai approach

This approach is also heavily used by the community to calculate the stiffness of unidirectional MWCNT-reinforced nanocomposite as a function of the aspect ratio of the nanofillers. In this method, based on the loading direction and filler geometry, Young's moduli are defined in the longitudinal and transverse independently [16]. Then, the overall Young's modulus of the nanocomposite is predicted using those two terms as follows [16,24]:

$$E=\frac{3}{8}E_L+\frac{5}{8}E_T, \tag{12}$$

in which the longitudinal E_L and transverse E_T Young's moduli are presented below [16,24]:

$$E_L=\frac{1+AR\cdot\eta_L\cdot f_r}{1-\eta_L\cdot f_r}E_m,\quad E_T=\frac{1+2\eta_T\cdot f_r}{1-\eta_T\cdot f_r}E_m, \tag{13}$$

where AR is the aspect ratio of nanofiller and

$$\eta_L=\frac{(E_r/E_m)-1}{(E_r/E_m)+AR},\quad \eta_T=\frac{(E_r/E_m)-1}{(E_r/E_m)+2}. \tag{14}$$

Moreover, the relation between the weight and volume fractions of MWCNT inside the polymer is as follows:

$$f_r=\frac{w_f}{w_f+\frac{\rho_r}{\rho_m}-\frac{\rho_r}{\rho_m}w_f}, \tag{15}$$

where ρ is the mass density.

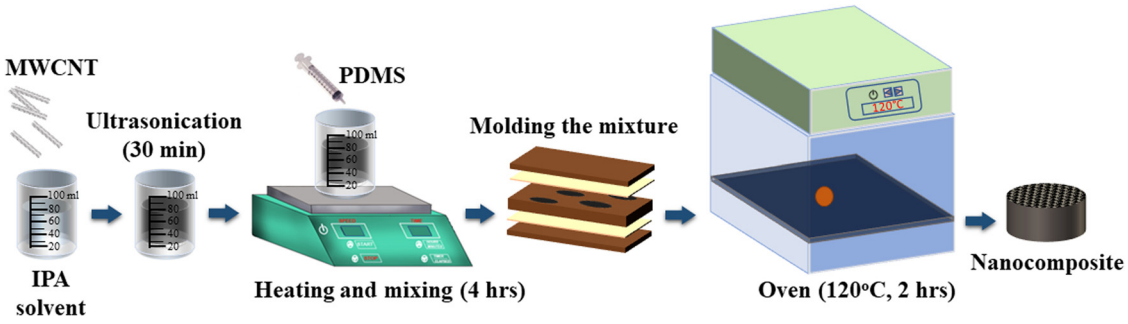

Figure 2: Schematic of the preparation process of PDMS/MWCNT nanocomposites.

3 Experimentation

3.1 Preparation of PDMS/MWCNT nanocomposite

Commercially available PDMS (Sylgard 184 two-component Dow Corning) and MWCNT (Shengzhen Nanotech Port Co. Ltd, average diameters: 9.5 nm, average length: 1.5 μm) were used as the polymer matrix and reinforcement particle, respectively, to fabricate the nanocomposite. In this study, PDMS/MWCNT nanocomposites with different MWCNT contents (*e.g.*, 0.1, 0.25, and 0.5 wt%) were fabricated by the solution casting technique. Figure 2 describes a schematic of the PDMS/MWCNT nanocomposite preparation process. At the beginning of the process, a certain amount of MWCNT was dispersed in isopropyl alcohol (IPA) by ultrasonication for 30 min [52]. Then, a specific amount of PDMS was inserted into the solution and was mixed by a magnetic stirrer for 4 h to completely extract the IPA. A polymer crosslinker (Sylgard, 1:10 weight ratio for PDMS to curing agent) was added to the mixture to help the polymer curing process. At the final step, the mixture was poured into the mold cavities (29 mm diameter, 13 mm thickness) and put in an oven at 120°C for 2 h to be cured. Figure 3 shows the fabricated pure PDMS and nanocomposite discs.

3.2 Characterization

The compression tests were conducted by Instron Universal testing machine (INSTRON 5944) under force control (0.2 mm/min) displacement mode [53]. The test was in accordance with the ASTM D1229 – 03 standard test method. Young's modulus of nanocomposites was concluded from the trendline slope of the linear elastic regions of the stress–strain curves obtained from the compression tests. Dispersion of MWCNT in the polymer matrix was observed by transmission electron microscope (TEM, Hitachi H7500), which was taken in the Center of Neurobiology of Stress at the University of Toronto Scarborough. For the sample preparation, samples were cut into small triangle pieces using a razor and then were mounted onto slotted pins from electron microscopy sciences (EMS) and sectioned (50 nm) at a temperature of –120°C using liquid nitrogen to cool the chamber and maintain the temperature.

4 Results and discussions

According to the procedure presented in Section 3, samples with different nanofiller fractions have been prepared. Figure 4 illustrates the TEM micrographs of the nanocomposite where the MWCNTs dispersion and

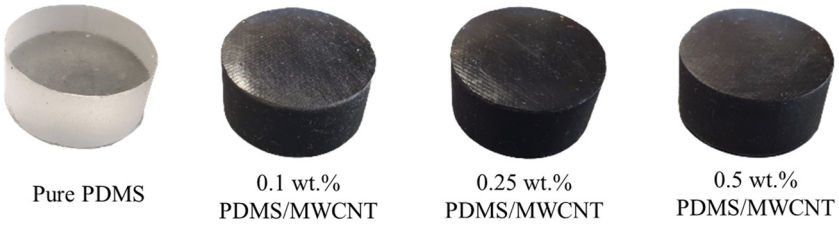

Figure 3: Actual fabricated samples: Pure PDMS and PDMS/MWCNT nanocomposites with different MWCNT contents.

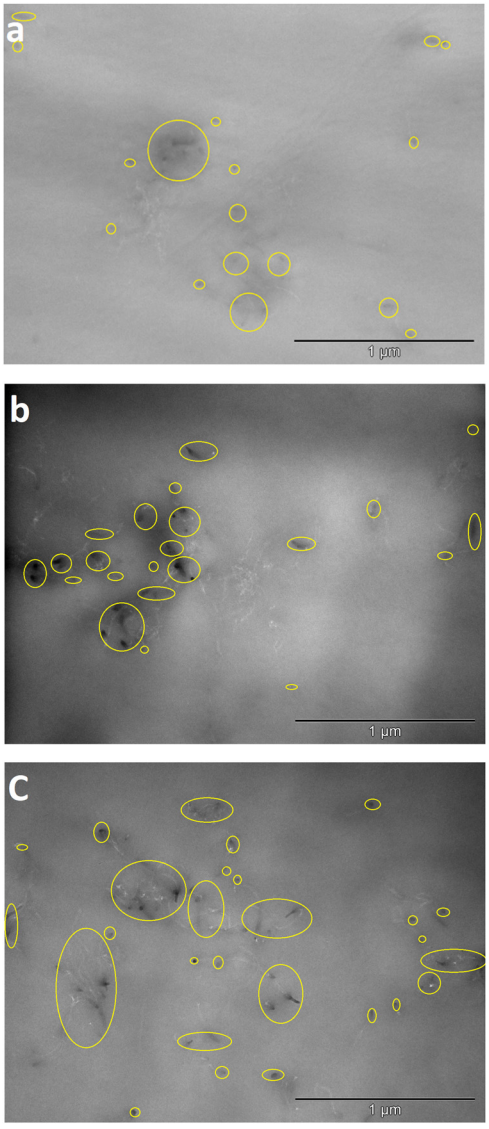

Figure 4: TEM micrographs of PDMS/MWCNT nanocomposite at (a) 0.1 wt% MWCNT content, (b) 0.25 wt% MWCNT content, and (c) 0.5 wt% MWCNT content. The yellow areas show MWCNT agglomeration.

particles agglomerations can be observed. According to these micrographs, MWCNT particles were not desirably dispersed in the polymer matrix and the nanofiller clusters increased by adding the MWCNT content in the nanocomposites. Figure 5 depicts the compressive stress *versus* compressive strain results from experimental compression tests. The experimental results indicated that adding MWCNT particles to the pure PDMS matrix noticeably enhanced its Young's modulus (slop of the graphs). Moreover, increasing the MWCNT content from 0.1 to 0.25 wt% improved the nanocomposite's modulus as well. However, at 0.5 wt% MWCNT, the elastic modulus of the nanocomposite did not significantly change in comparison to 0.25 wt%

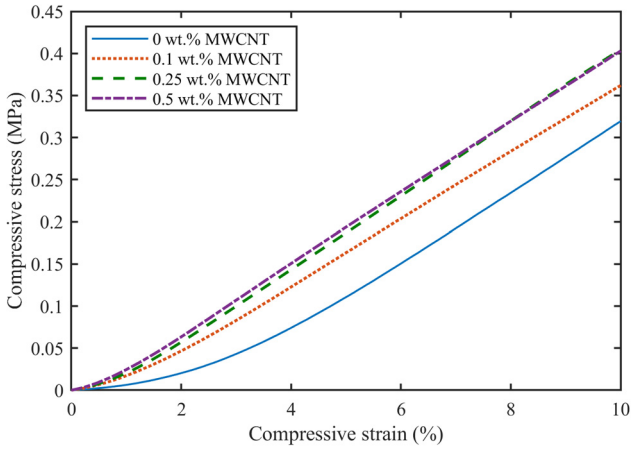

Figure 5: Compressive stress *vs* compressive strain graphs for PDMS/MWCNT nanocomposites with different MWCNT contents.

MWCNT content, which might be the result of increased agglomeration effect at higher filler content. Therefore, it can be concluded that high MWCNT agglomerations in the nanocomposite structure can adversely act as stress concentrators and decay the mechanical properties of the particle-reinforced composite.

Theoretical results have been calculated by considering E_r = 1 TPa, υ_r = 0.162, AR = 315.8, E_m = 3.53 MPa, and υ_m = 0.4. Figure 6 shows the calculated Young's moduli of PDMS/MWCNT nanocomposites obtained from both EMT and HT's approaches at different MWCNT weight fractions while they are compared with our experimental results. In view of HT results, we can see this approach suggesting a continual and almost linear relation between the embedded MWCNT content and Young's modulus, which has good agreements with measured results at

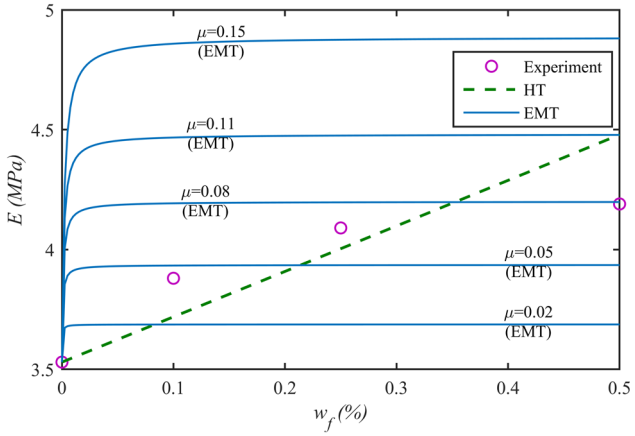

Figure 6: Young's modulus of PDMS/MWCNT nanocomposite obtained from HT, EMT (with different aggregation states), and experimental compression test *versus* MWCNT weight fraction.

low MWCNT contents. It means this approach properly estimates Young's modulus of PDMS/MWCNT nanocomposite when the nanocomposite contains low amounts of the nanofiller. However, HT fails to estimate the elasticity modulus of such nanocomposite at higher amounts of MWCNTs due to ignoring the effect of lumping these high aspect ratio nanofillers. Furthermore, the results of EMT's approach reveal that EMT is successful in predicting the effect of MWCNT agglomerations at the high amounts of w_f. However, this method estimates the formation of agglomerations at lower nanofiller contents rather than the experimental tests. According to this theoretical approach, the embedded MWCNTs are dispersed only in 8% of the volume of the resulting nanocomposite. This conclusion on the MWCNT dispersion can be verified by TEM micrographs, which are shown in Figure 4. As discussed before, it seems that EMT's approach reflects the effect of MWCNT agglomerations on the elasticity modulus at a smaller amount of filler contents rather than the experiment results. The reason behind this observation could be attributed to the soft inheritance of PDMS, which has a very low elasticity modulus (E_m = 3.53 MPa). Overall, Figure 6 indicates that both EMT's (with μ = 0.08) and HT's approaches estimate Young's modulus of PDMS/MWCNT nanocomposite with less than 8% error while $0 < w_f < 0.5\%$.

As HT's approach considers a shape parameter (nanofiller aspect ratio), Figure 7 examines the impact of this parameter on the estimated Young's modulus of PDMS/MWCNT nanocomposite for the four w_f used in the experimental tests. This figure reveals that the use of MWCNTs with higher aspect ratios results in stiffer nanocomposites. Moreover, it is observed that there is almost a linear relationship between the aspect ratio of nanofiller and elasticity

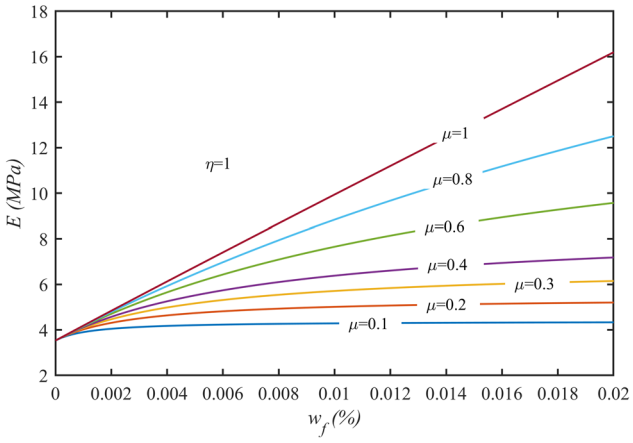

Figure 8: Young's modulus of PDMS/MWCNT nanocomposite obtained from EMT's approach *versus* MWCNT weight fraction for different MWCNT cluster sizes when η = 1.

modulus of the resulting nanocomposite in which the trends are steeper for the nanocomposites with a higher amount of MWCNTs.

In Figures 8 and 9, the effects of different MWCNT agglomerations on Young's modulus of PDMS/MWCNT nanocomposite are depicted using EMT's approach. Figure 8 reveals that enlarging MWCNT cluster sizes (higher μ), while all MWCNTs are located inside such clusters (η = 1), improves the elasticity modulus of the nanocomposites. Moreover, as expected, by increasing μ, the negative effect of MWCNTs lumping is postponed such that the comparison between the results of μ = 0.1 and μ = 0.4 shows this effect can be seen when $w_f > 0.004\%$ and $w_f > 0.02\%$, respectively. Figure 9 plots a comprehensive illustration of the impact of agglomeration states on Young's modulus of the

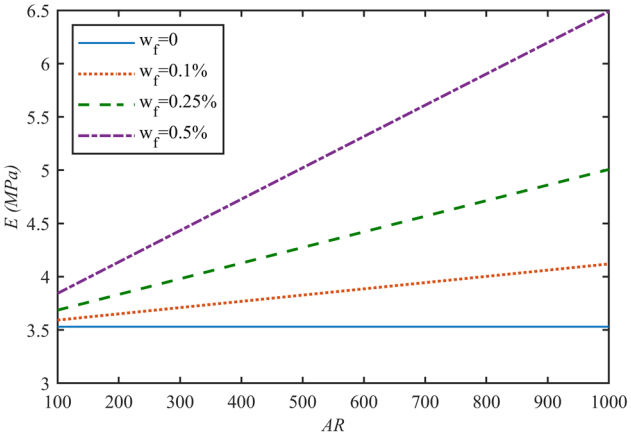

Figure 7: Young's modulus of PDMS/MWCNT nanocomposite obtained from HT approach *versus* MWCNT aspect ratio for different nanofiller weight fractions.

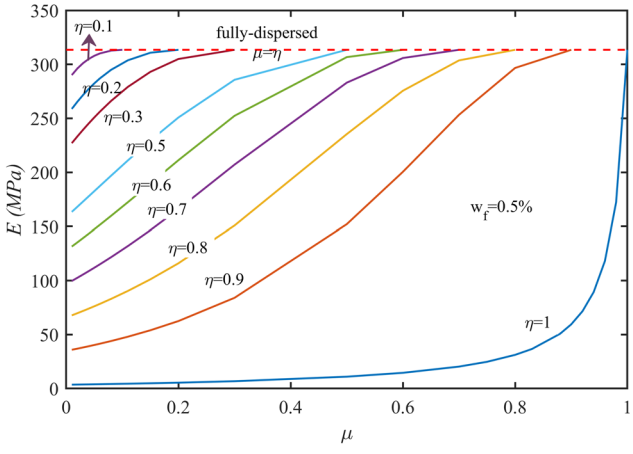

Figure 9: Young's modulus of PDMS/MWCNT nanocomposite obtained from EMT's approach *versus* MWCNT cluster sizes for different concentrations of MWCNTs inside clusters when w_f = 0.5%.

resulting nanocomposites by changing μ and η. A general observation of this figure shows that PDMS/MWCNT nanocomposites with agglomeration states describing with lower μ and higher η possess higher elasticity modulus due to MWCNT dispersion improvement inside the PDMS. Moreover, as expected, nanocomposites with the highest elasticity modulus can be achieved when $\mu = 1$ or $\mu = \eta$, which describes a nanocomposite with fully dispersed MWCNT in PDMS matrix.

5 Conclusion

In this article, the effect of MWCNT particles on Young's modulus of PDMS/MWCNT nanocomposite was investigated using experimental tests and two theoretical approaches including EMT and Halpin–Tsai. The comparison between the results of experimental and theoretical methods showed that the accuracy of HT's approach at lower MWCNT contents is higher than EMT's approach. However, EMT predicts the elastic modulus of PDMS/MWCNT nanocomposites at higher MWCNT contents more precisely due to considering the effect of MWCNT agglomerations. According to the experimental results, the presence of MWCNT particles in the PDMS matrix improved the mechanical strength of the nanocomposite, which was comprehended by the stress–strain graphs. Increasing the MWCNT content in the nanocomposites up to 0.25 wt% enhanced their Young's modulus. However, exceeding this content did not significantly improve Young's modulus, which can be the result of increased MWCNT clusters in the nanocomposite structure. To reduce the MWCNT agglomeration for the future work, some methods are recommended. Since increasing the ultrasonication time or amplitude creates powerful vibration waves, which results in the breakage of the tubes, an alternative way to better disperse the particles can be the use of high-speed disperser [54]. In the high-speed disperser, the high speed and minimal gap between the rotor and stator produced extremely strong shear forces, which results in better particle dispersion with less tube breakage. Moreover, adding surfactant to the MWCNT and solvent mixture can improve the particle dispersion as well. The formation of a layer of a surfactant coat on CNT surface helps to counterbalance van der Waals attractions between CNTs and results in the better particle dispersion [55].

The potential use of fabricated nanocomposite is for force mapping in biomedical applications. The tailored PDMS/MWCNT nanocomposite with 0.25 wt% MWCNT shows piezoresistive behaviors, which means its electrical resistance changes while an external force is applied to it, and therefore this nanocomposite can perform as a pressure sensor.

Funding information: The work described in this paper was supported by Natural Sciences and Engineering Research Council of Canada (NSERC under grant RGPIN-217525). The authors are grateful for their supports.

Author contributions: All authors have accepted responsibility for the entire content of this manuscript and approved its submission.

Conflict of interest: The authors state no conflict of interest.

References

[1] Amjadi M, Kyung KKU, Park I, Sitti M. Stretchable, skin-mountable, and wearable strain sensors and their potential applications: a review. Adv Funct Mater. 2016;26(11):1678–98.
[2] Chortos A, Liu J, Bao Z. Pursuing prosthetic electronic skin. Nat Mater. 2016;15(9):937–50.
[3] Park J, You I, Shin S, Jeong U. Material approaches to stretchable strain sensors. ChemPhysChem. 2015;16(6):1155–63.
[4] Moradi-Dastjerdi R, Behdinan K. Temperature effect on free vibration response of a smart multifunctional sandwich plate. J Sandw Struct Mater. 2021;23(6):2399–421. doi: 10.1177/1099636220908707.
[5] Zuruzi AS, Haffiz TM, Affidah D, Amirul A, Norfatriah A, Nurmawati MH. Towards wearable pressure sensors using multiwall carbon nanotube/polydimethylsiloxane nanocomposite foams. Mater Des. 2017;132:449–58.
[6] Iglio R, Mariani S, Robbiano V, Strambini L, Barillaro G. Flexible polydimethylsiloxane foams decorated with multiwalled carbon nanotubes enable unprecedented detection of ultralow strain and pressure coupled with a large working range. ACS Appl Mater Interfaces. 2018;10(16):13877–85.
[7] Karimzadeh S, Safaei B, Jen TC. Prediction effect of ethanol molecules on doxorubicin drug delivery using single-walled carbon nanotube carrier through POPC cell membrane. J Mol Liq. 2021 May 15;330:115698.
[8] Karimzadeh S, Safaei B, Jen TC. Investigate the importance of mechanical properties of SWCNT on doxorubicin anti-cancer drug adsorption for medical application: a molecular dynamic study. J Mol Graph Model. 2020;101:1–29.
[9] Meschino M, Wang L, Xu H, Moradi-Dastjerdi R, Behdinan K. Low-frequency nanocomposite piezoelectric energy harvester with embedded zinc oxide nanowires. Polym Compos. 2021;42:4573–85. doi: 10.1002/pc.26169.
[10] Ren X, Seidel GD. Computational micromechanics modeling of piezoresistivity in carbon nanotube-polymer nanocomposites. Compos Interfaces. 2013;20(9):693–720.
[11] Zare Y, Rhee KY. Two-stage simulation of tensile modulus of carbon nanotube (CNT)-reinforced nanocomposites after

percolation onset using the ouali approach. JOM. 2020;72(11):3943–51. doi: 10.1007/s11837-020-04223-3.
[12] Singh NP, Gupta VK, Singh AP. Graphene and carbon nanotube reinforced epoxy nanocomposites: a review. Polymer (Guildf). 2019 Oct 10 [cited 2019 Oct 4];180:121724. https://www.sciencedirect.com/science/article/pii/S003238611930730X.
[13] Pan S, Dai Q, Safaei B, Qin Z, Chu F. Damping characteristics of carbon nanotube reinforced epoxy nanocomposite beams. Thin-Walled Struct. 2021 Sep 1 [cited 2021 Aug 3];166:108127. https://linkinghub.elsevier.com/retrieve/pii/S0263823121004146.
[14] Barathi Dassan EG, Anjang Ab Rahman A, Abidin MSZ, Akil HM. Carbon nanotube-reinforced polymer composite for electromagnetic interference application: a review. Nanotechnol Rev. 2020;9(1):768–88.
[15] Moradi-Dastjerdi R, Radhi A, Behdinan K. Damped dynamic behavior of an advanced piezoelectric sandwich plate. Compos Struct. 2020;243:112243. doi: 10.1016/j.compstruct.2020.112243.
[16] Kundalwal SI. Review on micromechanics of nano- and microfiber reinforced composites. Polym Compos. 2018;39(12):4243–74. doi: 10.1002/pc.24569.
[17] Fitzgerald G, DeJoannis J, Meunier M. Multiscale modeling of nanomaterials: recent developments and future prospects. Modeling, characterization and production of nanomaterials: electronics, photonics and energy applications. Vol. 3. Woodhead Publishing; 2015. p. 53. doi: 10.1016/B978-1-78242-228-0.00001-6.
[18] Liu WK, Karpov EG, Zhang S, Park HS. An introduction to computational nanomechanics and materials. Computer Methods in Appl Mech Eng. 2004;193(17–20):1529–78. doi: 10.1016/j.cma.2003.12.008.
[19] Shen H. Nonlinear bending of functionally graded carbon nanotube-reinforced composite plates in thermal environments. Compos Struct. 2009;91(1):9–19. doi: 10.1016/j.compstruct.2009.04.026.
[20] Martone A, Faiella G, Antonucci V, Giordano M, Zarrelli M. The effect of the aspect ratio of carbon nanotubes on their effective reinforcement modulus in an epoxy. Compos Sci Technol. 2011;71(8):1117–23. doi: 10.1016/j.compscitech.2011.04.002.
[21] Moradi-Dastjerdi R, Pourasghar A. Dynamic analysis of functionally graded nanocomposite cylinders reinforced by wavy carbon nanotube under an impact load. J Vib Control. 2016;22:1062–75.
[22] Moradi-Dastjerdi R, Payganeh G, Tajdari M. Resonance in functionally graded nanocomposite cylinders reinforced by wavy carbon nanotube. Polym Compos. 2017;38:E542–52.
[23] Moradi-Dastjerdi R, Payganeh G, Tajdari M. Thermoelastic analysis of functionally graded cylinders reinforced by wavy CNT using a mesh-free method. Polym Compos. 2018;39(7):2190–201.
[24] Shokrieh MM, Rafiee R. Investigation of nanotube length effect on the reinforcement efficiency in carbon nanotube based composites. Compos Struct. 2010;92:2415–20.
[25] Moradi-Dastjerdi R, Meguid SA, Rashahmadi S. Electrodynamic analysis of smart nanoclay-reinforced plates with integrated piezoelectric layers. Appl Math Model. 2019;75:267–78. doi: 10.1016/j.apm.2019.05.033.
[26] Shi D, Feng X, Huang YY, Hwang K-C, Gao H. The effect of nanotube waviness and agglomeration on the elastic property of carbon nanotube- reinforced composites. J Eng Mater Technol. 2004;126(July):250–7.
[27] Moradi-Dastjerdi R, Behdinan K. Free vibration response of smart sandwich plates with porous CNT-reinforced and piezoelectric layers. Appl Math Model. 2021;96:66–79. doi: 10.1016/j.apm.2021.03.013.
[28] Moradi-Dastjerdi R, Behdinan K. Dynamic performance of piezoelectric energy harvesters with a multifunctional nanocomposite substrate. Appl Energy. 2021;293:116947. doi: 10.1016/j.apenergy.2021.116947.
[29] Montazeri A, Javadpour J, Khavandi A, Tcharkhtchi A, Mohajeri A. Mechanical properties of multi-walled carbon nanotube/epoxy composites. Mater Des. 2010;31(9):4202–8. doi: 10.1016/j.matdes.2010.04.018.
[30] Barai P, Weng GJ. A theory of plasticity for carbon nanotube reinforced composites. Int J Plast. 2011;27(4):539–59. doi: 10.1016/j.ijplas.2010.08.006.
[31] Krishnaswamy AJ, Buroni FC, Garcia-Sanchez F, Melnik R, Rodriguez-Tembleque L, Saez A. Lead-free piezocomposites with CNT-modified matrices: Accounting for agglomerations and molecular defects. Compos Struct. 2019;224(April):111033.
[32] Lu J, Lu M, Bermak A, Lee YK. Study of piezoresistance effect of carbon nanotube-PDMS composite materials for nanosensors. 2007 7th IEEE International Conference on Nanotechology: IEEE-NANO 2007 Proceedings; 2007. p. 1240–3.
[33] Chandel VS, Wang G, Talha M. Advances in modelling and analysis of nano structures: a review. Nanotechnol Rev. 2020;9(1):230–58.
[34] Tanabi H, Erdal M. Effect of CNTs dispersion on electrical, mechanical and strain sensing properties of CNT/epoxy nanocomposites. Results Phys. 2019;12(1):486–503.
[35] Madaleno L, Pyrz R, Crosky A, Jensen LR, Rauhe JCM, Dolomanova V, et al. Composites: part A processing and characterization of polyurethane nanocomposite foam reinforced with montmorillonite – carbon nanotube hybrids. Compos Part A. 2013;44:1–7.
[36] Montinaro N, Fustaino M, Pantano A. Carbon nanotubes dispersion assessment in nanocomposites by means of a pulsed thermographic approach. Materials (Basel). 2020;13(24):1–13.
[37] Ma PC, Siddiqui NA, Marom G, Kim JK. Dispersion and functionalization of carbon nanotubes for polymer-based nanocomposites: a review. Compos Part A Appl Sci Manuf. 2010;41(10):1345–67.
[38] Siddiqui NA, Li EL, Sham ML, Tang BZ, Gao SL, Mäder E, et al. Tensile strength of glass fibres with carbon nanotube-epoxy nanocomposite coating: effects of CNT morphology and dispersion state. Compos Part A Appl Sci Manuf. 2010;41(4):539–48.
[39] Zhou YX, Wu PX, Cheng ZY, Ingram J, Jeelani S. Improvement in electrical, thermal and mechanical properties of epoxy by filling carbon nanotube. Express Polym Lett. 2008;2(1):40–8.
[40] Schilde C, Schlömann M, Overbeck A, Linke S, Kwade A. Thermal, mechanical and electrical properties of highly loaded CNT-epoxy composites – a model for the electric conductivity. Compos Sci Technol. 2015;117:183–90.
[41] Wagner HD, Lourie O, Feldman Y, Tenne R. Stress-induced fragmentation of multiwall carbon nanotubes in a polymer matrix. Appl Phys Lett. 1998;72(2):188–90.
[42] Park SB, Lih E, Park KS, Joung YK, Han DK. Biopolymer-based functional composites for medical applications. Prog Polym Sci. 2017;68:77–105.
[43] Wang JK, Xiong GM, Zhu M, Özyilmaz B, Castro Neto AH, Tan NS, et al. Polymer-enriched 3D graphene foams for biomedical applications. ACS Appl Mater Interfaces. 2015;7(15):8275–83.

[44] Kaur G, Adhikari R, Cass P, Bown M, Gunatillake P. Electrically conductive polymers and composites for biomedical applications. RSC Adv. 2015;5(47):37553–67.
[45] Lee W, Hong S. Characterization of elastic polymer-based smart insole and a simple foot plantar pressure visualization method using 16 electrodes. Sensors. 2019;19:1–10.
[46] Kim K, Hong SK, Jang N, Ha S, Lee HW, Kim J. Wearable resistive pressure sensor based on highly flexible carbon composite conductors with irregular surface morphology. ACS Appl Mater Interfaces. 2017;9:17499–507.
[47] Wang M, Guo Z. Enhanced electrical conductivity and piezoresistive sensing in multi-wall carbon nanotubes/polydimethylsiloxane nanocomposites *via* the construction of a self-segregated structure. R Soc Chem. 2017;9(31):11017–26.
[48] Hammock ML, Chortos A, Tee BCK, Tok JBH, Bao Z. 25th Anniversary article: The evolution of electronic skin (E-Skin): a brief history, design considerations, and recent progress. Adv Mater. 2013;25(42):5997–6038.
[49] Li M, Li H, Zhong W, Zhao Q, Wang D. Stretchable conductive polypyrrole/polyurethane (PPy/PU) strain sensor with netlike microcracks for human breath detection. ACS Appl Mater Interfaces. 2014;6(2):1313–9.
[50] Eshelby JD. The determination of the elastic field of an ellipsoidal inclusion, and related problems. Proc R Soc London Ser A. 1957;241:376–96.
[51] Mura T. Micromechanics of defects in solids. The Hague: Martinus Nijhoff Pub; 1982.
[52] Roy S, Petrova RS, Mitra S. Effect of carbon nanotube (CNT) functionalization in epoxy-CNT composites. Nanotechnol Rev. 2018;7(6):475–85.
[53] Ghahramani P, Eldyasti A, Leung SN. Open-cell polyvinylidene fluoride foams as carriers to promote biofilm growth for biological wastewater treatment. Polym Eng Sci. 2021 Aug 1 [cited 2021 Aug 13];61(8):2161–71. doi: https://onlinelibrary.wiley.com/doi/full/10.1002/pen.25741.
[54] Paton KR. Scalable production of large quantities of defect-free few-layer graphene by shear exfoliation in liquids. Nat Mater. 2014;13:624–30.
[55] Cui H, Yan X, Monasterio M, Xing F. Effects of various surfactants on the dispersion of MWCNTs – OH in aqueous solution. Nanomaterials. 2017;7:262.